12th International Symposium on Turbulence and Shear Flow Phenomena (TSFP12)
Osaka, Japan (Online), July 19-22, 2022

IMPLICATIONS OF SHEAR AND THERMAL STRATIFICATION ON WIND TURBINE TIP-VORTEX STABILITY

Amy Hodgkin
Turbulence Simulation Group
Department of Aeronautics
Imperial College London
London SW7 2AZ, UK
a.hodgkin19@imperial.ac.uk

Sylvain Laizet
Turbulence Simulation Group
Department of Aeronautics
Imperial College London
London SW7 2AZ, UK
s.laizet@imperial.ac.uk

Georgios Deskos
National Wind Technology Center
National Renewable Energy Laboratory
Golden, Colorado, 80401, USA
georgios.deskos@nrel.gov

ABSTRACT

The interaction between wind turbines in a wind farm through their wakes is a phenomenon that has been studied for decades and is still relevant today. Turbines clustered together in arrays will often operate in the wake of other upstream turbines which may lead to significant power losses and fatigue loads. For modern large-scale wind turbines, the mean shear velocity profile and thermal stratification are major components of the atmospheric boundary layer so it is important to understand their impact on near-wake development. Additionally, veer is present due to the rotation of the Earth. The impact of shear, thermal stratification and veer on the stable wake length of turbines with a dynamic control strategy is studied numerically in this work using a suite of highly resolved large-eddy simulations. Instantaneous flow fields are extracted from the simulations and used to conduct proper orthogonal decomposition (POD) and compute the mean kinetic energy fluxes by different POD modes to better understand the tip-vortex instability mechanisms. Our findings show that the dynamic pitch control scheme is able to shorten the stable wake length to about $1.5R$ in uniform flow. Shear can significantly affect the break up of wind turbine tip-vortices as well as the shape and stable length of the wake, whereas thermal stratification seems to only have limited contribution to the spatial development of the near-wake field. Veer causes the wake boundary to skew but has a limited impact on the wake length.

INTRODUCTION

Wind turbines operate in large-scale farms where the wake of turbines interact with each other. A turbine's wake has a velocity deficit and impacts the turbulence intensity, therefore turbines which sit within a wake experience reductions in power generation reported to be in the order of 10-25% and increases in fatigue loads of a similar magnitude (Barthelmie *et al.*, 2010; Hansen *et al.*, 2012). The interaction between atmospheric turbulence and turbine wakes is complex so decomposing flow phenomena to understand the impact of different components of the atmospheric boundary layer (ABL) is useful. In particular, wind turbines which exist high up in the ABL can be subjected to strong shear and thermal stratification which vary in strength throughout the day. Thermal stratification impacts the shear profile and the intensity and structure of turbulence. The thermal stratification gradient can be used to classify the ABL into neutral, stable and convective. When the thermal stratification is positive, the boundary layer is considered to be stable. In the stable boundary layer the wake has been found to be the longest, with the highest reductions in power output, so is of particular interest (Abkar & Porté-Agel, 2015). Hodgkin *et al.* (2022) conduct thorough analysis on wakes in a comprehensive range of shear and thermal stratification strengths. They find that shear has a large impact on the wake length and shape and breakdown locations, whereas thermal stratification only has a limited effect on the wake shape. Additionally, due to Coriolis forces caused by the rotation of the Earth, wind turbines can be subjected to veer, where the direction of the wind changes with height. This can be especially significant in stable conditions, causing the wind turbine wake to skew (Churchfield & Sirnivas, 2018). By studying the mean kinetic energy (MKE) flux across the wake, Lignarolo *et al.* (2015) find that the helical tip-vortices of the wake inhibit turbulent mixing and prevent transition to turbulence. Therefore, the wake will not break down without an additional disturbance.

The stable wake length is a key parameter in wind farm optimisation. Knowledge of the mechanisms that cause wake breakdown can improve farm efficiency and design. The stable wake length can be defined as the length between the turbine rotor plane and the location where the wake's tip-vortex structure begins to break up into turbulence. The near-wake field transitions into the far-wake field as the tip-vortices break down into smaller turbulent structures which mix with the ambient fluid as the wake recovers (Vermeer *et al.*, 2003). Widnall (1972) states that the mutual inductance instability is one of three main instabilities that leads the vortex breakdown. It occurs when out-of-phase perturbations causes neighbouring vortex filaments to disturb each other leading to vortex pairing and breakdown.

Control methods which aim to shorten the stable wake length by manipulating a turbine's induction factor, known as dynamic induction control, are growing in popularity. Using periodic fluctuations in torque or blade pitch, the thrust coefficient of a wind turbine can be altered in a way to enhance wake mixing. Munters & Meyers (2018*a*) find the optimal frequency for the perturbation has a Strouhal number of 0.25. Frederik *et al.* (2020) test the periodic scheme of Munters & Meyers (2018*a*) using pitch control in wind tunnel and large-eddy simulation (LES) experiments and confirm their findings, showing a potential power increase of up to 4% (mostly coming from the first downstream turbine). Brown *et al.* (2021) identify two optimal forcing strategies, one of which is to force the mutual induction instability, with a frequency equal to one and a half times the rotation rate. The optimal frequency for dynamic induction control is expected to depend on the turbine and atmospheric conditions, and the physical mechanisms which are responsible for the wake's breakdown need to be investigated in depth (Houck, 2022).

In this work, the breakup mechanisms of wind turbine tip-vortices in flow with shear, thermal stratification and veer are investigated using high-fidelity turbulence resolving simulations, with a focus on the near-wake field. We study impact of dynamic pitch control on the wake length and shape in these conditions. Data-driven analysis methods such as proper orthogonal decomposition and mean kinetic energy flux are utilised to further understand the role coherent structures have on the wake's breakdown.

METHOD

The high-fidelity turbulence resolving simulations in this work are carried out with the wind farm simulator `WInc3D` (Deskos *et al.*, 2020), which is part of the high-order, finite-difference, framework of flow solvers `Xcompact3d` (Bartholomew *et al.*, 2020). The simulations are based on the incompressible Navier-Stokes and temperature scalar transport equations, coupled through a gravitational term,

$$\frac{\partial u_i}{\partial x_i} = 0, \tag{1a}$$

$$\frac{\partial u_i}{\partial t} = -\frac{1}{2}\left(u_j\frac{\partial u_i}{\partial x_j} + \frac{\partial u_i u_j}{\partial x_j}\right) - \frac{\partial p}{\partial x_i} + \frac{1}{Re}\mathscr{D} + F_i, \tag{1b}$$

$$\frac{\partial \theta}{\partial t} = -u_j\frac{\partial \theta}{\partial x_j} + \frac{1}{Re\cdot Sc}Q, \tag{1c}$$

where u_i is the velocity vector field, p is the pressure field, θ is the potential temperature and F_i accounts for additional forcing (with $i = 1,2,3$ corresponding to the streamwise (x), vertical (y) and spanwise (z) directions, respectively), $Re = U_0R/\nu$ is the Reynolds number based on the reference free-stream velocity (U_0), the turbine radius (R) and the kinematic viscosity (ν), and Sc is the Schmidt number. These equations are solved with sixth-order finite-difference schemes on a Cartesian mesh. More details of the code implementation can be found in Laizet & Lamballais (2009); Laizet & Li (2011). Subgrid stresses are handled with an implicit LES scheme which uses the hyper-viscous momentum diffusion term ($\mathscr{D}$) or temperature diffusion term (Q) to introduce the required dissipation; more details can be found in Dairay *et al.* (2017). A conventional actuator line method is used to model the turbine via a forcing term added to the momentum equation.

The simulations setup is based on a scale-model three-bladed turbine (with radius $R = 10.24$ m) from experiments conducted in the wind-tunnel of NTNU (Krogstad & Eriksen, 2013). The computational domain, $10R\times 10R\times 10R$, is discretised with a uniform mesh of $513\times 513\times 513$ nodes. The turbine is placed at mid-height, $2R$ downstream of the inlet. The Reynolds number is equal to $Re = 30,000$ with a tip speed ratio, $\lambda = \omega_t R/U_0 = 6$, where ω_t is the angular velocity of the turbine.

The effect of shear and thermal stratification on the flow is studied by imposing vertical positive gradients of streamwise velocity and temperature. The velocity gradient is maintained with free-slip boundaries in the spanwise and vertical direction with inflow/outflow boundaries in the streamwise direction. The temperature gradient is maintained with vertical wall fixed-temperature boundary conditions. The strength of these gradients is defined as a percentage change in the quantity from the centre-line of the turbine ($y = 0$) to one vertical radius ($y = R$). We test shear strengths of 10%, 20% and 30% and thermal stratification of 1%. To study veer we alter the wind-direction by a constant 4° change in flow angle per vertical radius and maintain this using periodic boundary condition in the spanwise direction.

The method used to trigger tip-vortex instabilities is dynamic induction control, practically applied by altering the pitch of the blades. The pitch of the blades are defined in time with a sinusoidal function, $\theta_b = A\sin(\omega_t+\omega_e)t$, where θ_b is the pitch of blade b, ω_e is the excitation angular frequency, and A is the amplitude. This work follows previous recommendations (Munters & Meyers, 2018*b*; Frederik *et al.*, 2020) to have a low excitation frequency of $\omega_e \approx \omega_t/10$ and with an amplitude of 2.5°.

Proper orthogonal decomposition is an analysis technique that finds coherent structures of a flow field by finding orthogonal basis vectors which can be reconstructed to return to the complete flow field using

$$u_i = \overline{u}_i + \sum_{k=1}^{N}\phi_i^k a_k, \tag{2}$$

where $\bar{\cdot}$ indicates the averaged value over N snapshots, index k corresponds to the k^{th} mode velocity field, ϕ_i^k is the velocity of mode k in direction i and a_k is the corresponding temporal coefficient (amplitude). The modes are ordered in terms of their total energy contribution to the flow, and appear in pairs with the same frequency, shape and energy content.

The mean kinetic energy (MKE) flux can be used to quantify the impact that coherent structures have on the wake breakdown. A positive MKE flux indicates that the flow helps the wake break down, as this refers to turbulent energy being brought into the control volume from the ambient, whereas a negative MKE flux is the opposite, and hence suggests it is delaying breakdown. The MKE term is extracted from the transport equation for the MKE:

$$-\frac{\partial}{\partial x_j}\left(\overline{u}_i\overline{u_i'u_j'}\right), \tag{3}$$

with $\overline{u_i'u_j'} = \overline{u_iu_j} - \overline{u}_i\overline{u}_j$. To relate this to a specific POD mode the following approximation is used:

$$\overline{u_i'u_j'} \approx \overline{\sum_{k=1}^{N}(a_k\phi_i^k)\sum_{l=1}^{N}(a_l\phi_i^l)} = \sum_{k=1}^{N}\sum_{l=1}^{N}\overline{a_ka_l}\phi_i^k\phi_j^l = \sum_{k=1}^{N}\lambda_k\phi_i^k\phi_j^k, \tag{4}$$

where λ_k is the eigenvalue of mode k, which represents the strength of the k^{th} mode. Combining equation 3 and 4 and integrating this term over a control volume (V_c) enclosed by a surface (S_c) finds the turbulent MKE flux per unit area for a single mode:

$$\mathscr{F}_T^k = \frac{1}{S_c}\int_{V_c} -\frac{\partial}{\partial x_j}\left(\overline{u}_i\lambda_k\phi_i^k\phi_j^k\right)dV_c. \tag{5}$$

The MKE flux of a mode pair is simply the addition of the MKE flux for each mode in that pair. This method is explained in more depth in Hodgkin *et al.* (2022).

RESULTS

Uniform Flow

The wake from a turbine in uniform flow with dynamic pitch control can be seen in Figure 1. The stable wake length is about $1.5R$ and multiple 'overlap' locations can be seen where the vortex filaments have rolled over each other and interacted. Breakdown ultimately occurs when neighbouring vortex filaments, which oscillate partially out-of-phase, interact causing their perturbations to grow. The vortex interaction pattern caused by the selected excitation frequency can be seen more clearly in Figure 2. This plot shows the vortex filaments if they are cut along the top and flattened out so that $0°$ corresponds to the top of the domain and $180°$ to the bottom. The interaction sees vertical 'overlap' locations which are spaced approximately 0.7R apart and become more turbulent as they progress downstream.

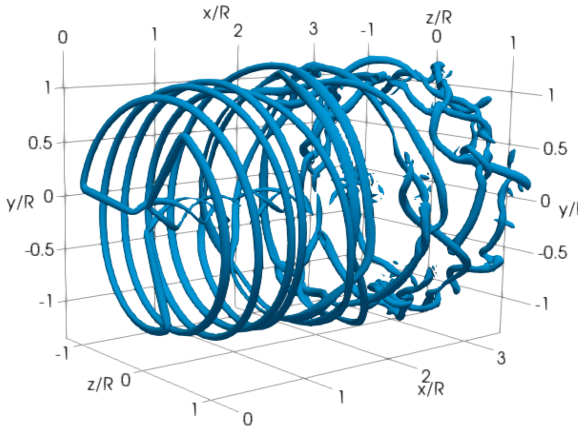

Figure 1. Vorticity contour of the wake in uniform flow with dynamic pitch control from $x = 0$ to $x = 3.5R$

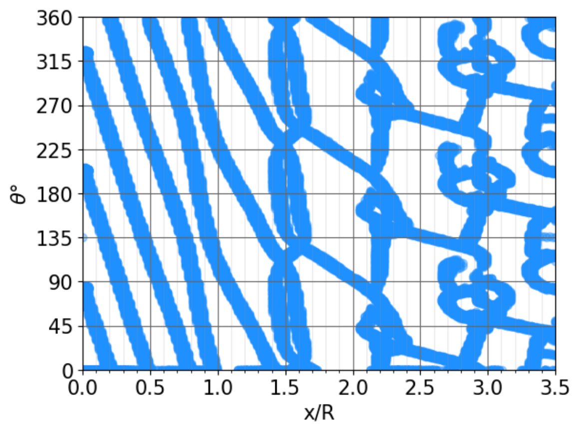

Figure 2. Planar vortex of the wake in uniform flow with dynamic pitch control from $x = 0$ to $x = 3.5R$

Shear

Shear acts to lengthen the wake along its top and shorten it along its bottom. This can be visualised by looking at the vorticity contours, in Figure 3, which show the wake as it expands downstream of the turbine for 10%, 20% and 30% shear. With shear, the spacing between neighbouring vortex filaments is increased along the top and reduced along the bottom, which consequently causes the wake to break down first at the bottom. Increasing shear increases the lengthening effect at the top and the shortening effect at the bottom. Turbulent structures are seen at the bottom of the domain once the wake has started to break down. We can look at the planar vortex lines to observe the vortex filament pattern more clearly. Figure 4 shows these for the 20% shear only case (as well as for 20% shear with and without thermal stratification and veer, discussed subsequently) . It can be seen that, although shear causes the vortex filaments to bend, there remains 'overlap' locations where the wake is breaking down. The first overlap is located at $x = 1.9R$ for $0°$ and at $x = 1.2R$ for $180°$. Shear increases the power extracted from the wind. The power coefficient compared with uniform flow increases by 0.22% for 10% shear, 0.78% for 20% shear and 1.56% for 30% shear.

Thermal Stratification

Thermal stratification is added to the 20% shear case to mimic the shear and thermal stratification levels in a stable boundary layer (Abkar & Porté-Agel, 2015). In a stable boundary layer strong shear is expected with a positive temperature gradient. Hodgkin *et al.* (2022) shows that the effect of thermal stratification is amplified with strong shear so this set up is the most interesting. There is little visible difference between the flow with and without thermal stratification. Thermal stratification alone does not change the location of the vortex breakdown. There is a slight advance in the breakup location with thermal stratification but this is negligible, shown in Figure 4. Thermal stratification reduces the power extracted from the wind. Adding 1% thermal stratification to 20% shear reduces the power coefficient compared with uniform flow to -1.01%, a 1.79% reduction from the 20% shear only case.

Veer

For interest, we add a constant veer gradient to the inflow with shear and thermal stratification. Veer is caused by the Earth's rotation and may have an impact on the wake length and shape. As seen in Figure 4 veer does not change the location of the vortex breakup or the stable wake length significantly. The power coefficient compared with uniform flow is reduced to -1.13%, a -0.12% reduction compared with the 20% shear + 1% thermal stratification case. This is small compared with the changes caused by adding thermal stratification or shear.

Wake Area

The wake area can be impacted by the simulation conditions. Figure 5 shows the boundary of the wake, calculated as the convex hull of the points which have a vorticity above a minimum average vorticity. The wake boundary is provided for 3 downstream locations, spaced $1R$ apart. For all cases the wake expands as it moves downstream. The uniform flow case has an equal radius for all angles about the turbine, of $1.26R$ at $3R$ downstream. Adding shear reduces the radius at $0°$ (top), at $3R$ this reduction is 3% for 10% shear, 5% for 20% shear and 12% for 30% shear. Shear increases the radius at the bottom, at $3R$ this increase is 4% for 10% shear, 9% for 20% shear and 19% for 30% shear. The change due to shear at the bottom is larger than at the top. Thermal stratification mainly has a impact on the radius at the sides, most clearly seen at $3R$. The radius at the sides is increased on average by 4% compared

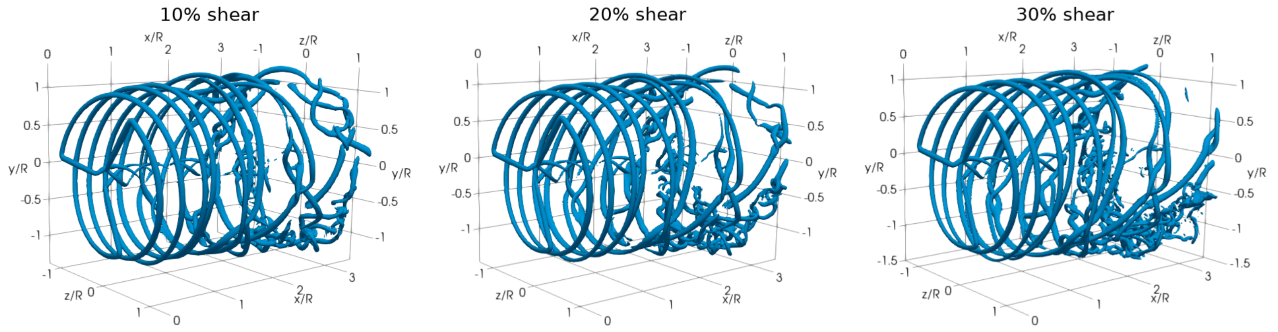

Figure 3. Vorticity contours of the wake in 10, 20 and 30% shear with dynamic pitch control from $x = 0$ to $x = 3.5R$

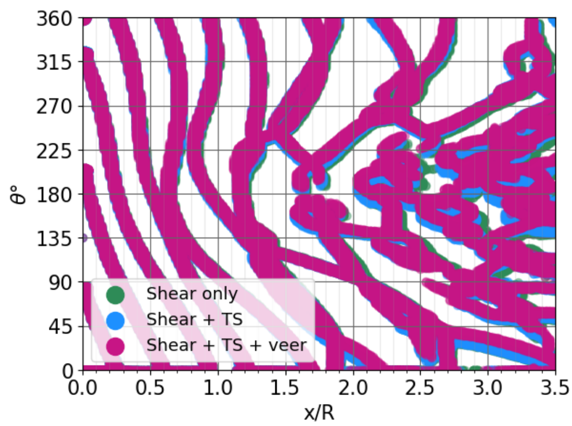

Figure 4. Planar vortex for cases with 20% shear with and without thermal stratification (TS) and veer from $x = 0$ to $x = 3.5R$

with the 20% shear only case. This change is comparable to the top and bottom effect caused by 10% shear. The most dramatic change to the wake boundary is observed when veer is present. Veer causes the wake boundary to skew, with maxima found at 45° and 225°. The location of the maximum radius for $3R$ (at 225°) is 8% bigger than the maximum radius found for the same case without veer (at 180°). The wake area could have a significant follow on impact to the far-wake field and dynamics.

Coherent Structures

We use POD to extract coherent structures from the flow field. The first mode of the four most dominant mode pairs for uniform flow are shown in Figure 6. The first three mode pairs are related to the control scheme, as these modes are not present when there is no control. The dominant frequency of mode pair 1 is the same as the pitch control frequency, $1.1w_t$, and distinct rings can be seen. Mode pair 4 is related to the helical spiral and is dominant in the first half of the domain when the wake in laminar or transitioning.

The four dominant POD mode shapes for 20% shear are shown in Figure 7. The mode frequencies and structure are the same as for uniform flow, but the modes are slanted to due to the effects of shear. In uniform flow, mode pair 1 extends through the whole domain, whereas in shear this mode maps onto the laminar part of the wake only, ending by $1.5R$ at the bottom of the domain. The shape of mode pair 2 also maps onto the laminar wake only, with its main structure ending at about $2.2R$ in uniform flow and $1.5R$ (bottom) and $3.5R$ (top) in sheared flow. Mode pair 4, which represents the helical spiral is dominant in the same parts of the domain as mode pair 2 for both inflows. Mode pair 3 on the other hand, begins once the wake starts to break down to turbulence, becoming strong by about $1.5R$ in uniform flow and $1R$ (bottom) and $2.5R$ (top) in shear flow. We note that mode pair 1 can be characterised as an anomaly in that it maps slightly differently for uniform and shear flow. The POD modes for the cases with thermal stratification and veer have the same structure as with uniform flow and shear only flow, and only their area and length shapes change slightly to map the overall shape of the wake.

Mean Kinetic Energy Flux

We calculate the total MKE flux for the four most dominant POD mode pairs ($\frac{\partial}{\partial x_j}\left(\overline{u}_i \lambda_k \phi_i^k \phi_j^k\right)$), as well as for the complete flow ($-\frac{\partial}{\partial x_j}\left(\overline{u}_i \overline{u_i' u_j'}\right)$). The control volume for the calculation is a cylinder, centred on the turbine, of radius $1.2R$ and length spanning from $x = 0.5R$ to $x = 3.5R$. The MKE flux values are normalised by the total MKE flux for the complete flow in uniform inflow. It is important to note that the wake area for each setup is different (Figure 5) so the control volume will be crossing the wake boundary at different points which can affect the results. However, we fix the boundary radius at $1.2R$ to account for some expansion of the wake. The data are shown in Figure 8. 10% shear and 20% shear cases both have a larger complete flow MKE flux than the uniform case, with the largest MKE flux at 20% shear (101% of uniform), however for 30% shear the MKE flux is about 90% of the uniform value. The wake radius at the bottom of the domain for 30% shear is much larger so this could be responsible for the reduction in flux, at least in part. Adding thermal stratification to 20% shear reduces the total MKE flux to just below 100%. The lowest MKE flux for complete flow (86% of uniform) is found for the case with thermal stratification and veer. However, as shown in Figure 4, veer does not reduce the stable wake length which indicates this difference could be related to the wake area rather than a true reduction in MKE flux.

Changing the inflow conditions has an impact on the total MKE flux in the four studied mode pairs. For all cases mode pair 4 relates to the helical spiral and has a negative MKE flux indicating that this mode pair delays wake recovery. This is expected as without any added disturbance the helical spiral vortex itself will not breakdown, as shown by Lignarolo *et al.* (2015). The magnitude of the MKE flux for mode pair 4 is largest for uniform flow, this suggests that the other inflow set ups reduce the shielding effect of the helical spiral. Shear, thermal stratification and veer all further reduce the magnitude of the MKE flux of this mode pair.

Mode pairs 1-3, which are related to the control strategy,

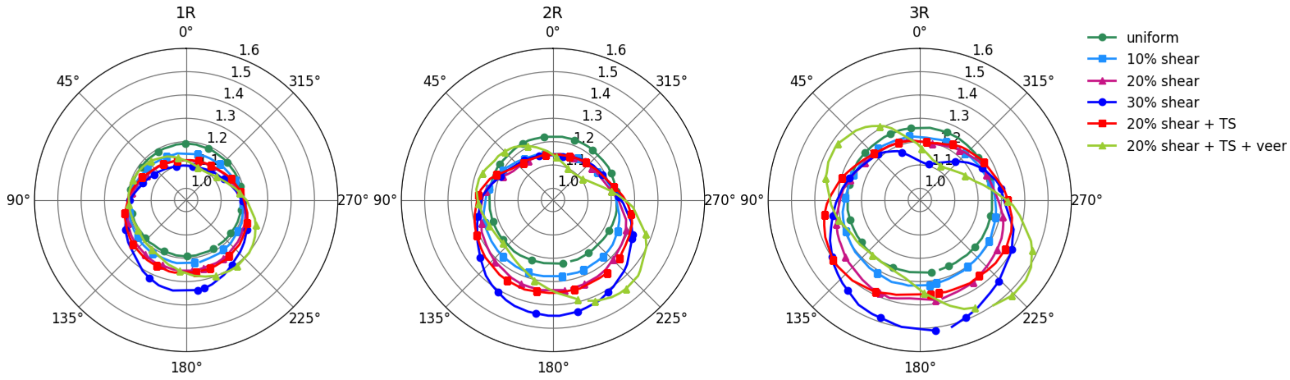

Figure 5. Plots showing the wake boundary for each case at three downstream locations, spaced 1R apart. *change last colour?

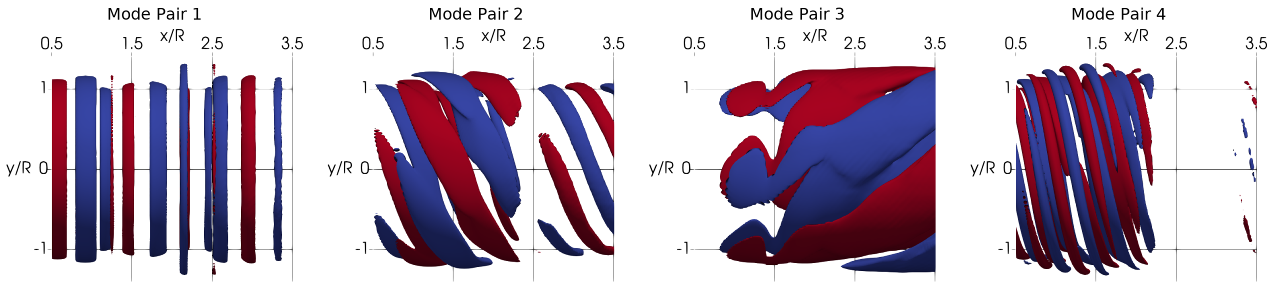

Figure 6. Four most dominant POD mode pair shapes for wake with dynamic pitch control in uniform flow

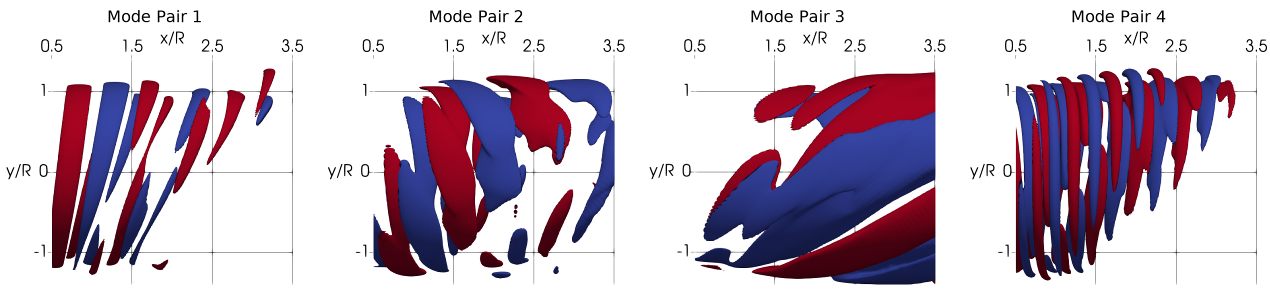

Figure 7. Four most dominant POD mode pair shapes for wake with dynamic pitch control in 20% shear flow

all have a positive MKE flux, hence they accelerate breakdown by providing the needed turbulent energy to disturb the wake's helical spiral structure. Mode pair 1 has the smallest flux for uniform flow and shear increases the flux of this mode, whereas, mode pairs 2 and 3 see the largest flux at uniform flow and shear decreases the flux for these modes. This means that mode pair 1 has the largest flux at 30% shear and it contributes the most to wake breakdown for this setup (out of the four studied modes). Thermal stratification slightly increases the flux in mode pair 1 and 3 but decreases the flux in mode pair 2. Adding veer decreases the flux in all 3 of these mode pairs. Veer dramatically changes the wake area which could be influencing this result.

For all cases, the MKE flux in the first four modes is in the order of a third of the complete flow MKE flux, suggesting that small scale turbulent structures (lower energy POD modes) contribute significantly to wake breakdown.

CONCLUSIONS

In this paper we have presented selected results from a set of simulations of a wind turbine with dynamic pitch control in flow with shear, thermal stratification and veer. The aim was to further understand how the dynamic pitch control is impacting the wake development in these flow conditions. We found that with dynamic pitch control, the stable wake length was shortened as vortex filaments were disturbed and interacted with each other by about 1.5R downstream of the turbine. With shear, the wake length is increased along the top and shortened along the bottom. This effect is more important when shear is increased. Thermal stratification alone does not impact the wake length significantly, but does reduce the power output from the turbine. For all cases, the wake expands as it travels downstream. In uniform flow the wake area is radially the same. The addition of shear decreases the radius at the top and increases it at the bottom. Thermal stratification causes an increase in the radius at the sides. The most noticeable impact from veer is a skew in the wake boundary shape, with a maximum effect found at 45° and 225°.

We found three dominant POD mode pairs relating to the pitch control, and the fourth most dominant was related to the helical spiral vortex. The four most dominant POD modes have the same structure for all inflow conditions, but their mode shape and area change to map onto the wake shape and

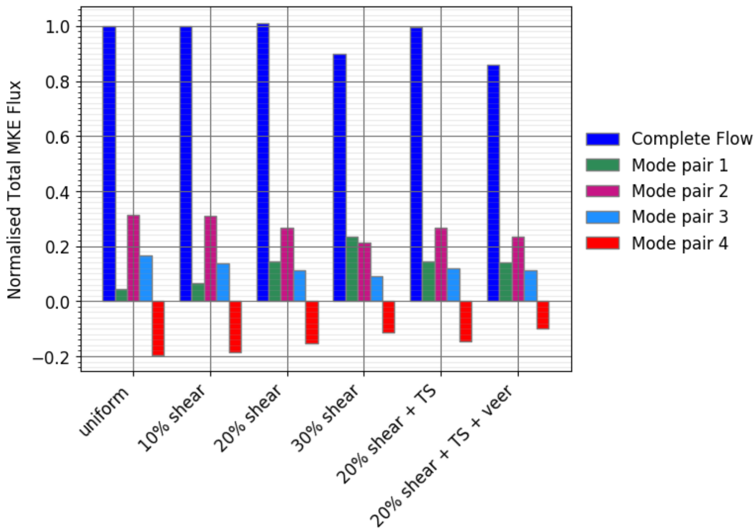

Figure 8. Total MKE flux for the first four POD mode pairs, normalised by the total MKE flux for the complete flow in uniform inflow.

area. Mode pairs 1-3 provide necessary MKE flux to cause wake breakdown and mode pair 4, which relates to the helical spiral vortex, provides a negative MKE flux. The magnitude of these fluxes is impacted by the inflow.

Future work will expand the analysis of these simulations using other decomposition methods based on frequency. We would then like to conduct simulations in a full turbulent boundary layer to see if these key conclusions hold in a more realistic configuration.

REFERENCES

Abkar, M. & Porté-Agel, F. 2015 Influence of atmospheric stability on wind-turbine wakes: A large-eddy simulation study. *Physics of fluids* **27** (3), 035104.

Barthelmie, R J, Pryor, S C, Frandsen, S T, Hansen, K S, Schepers, J G, Rados, K, Schlez, W, Neubert, A, Jensen, L E & Neckelmann, S 2010 Quantifying the impact of wind turbine wakes on power output at offshore wind farms. *Journal of Atmospheric and Oceanic Technology* **27** (8), 1302–1317.

Bartholomew, P., Deskos, G., Frantz, R., Schuch, F. N., Lamballais, E. & Laizet, S. 2020 Xcompact3d: An open-source framework for solving turbulence problems on a cartesian mesh. *SoftwareX* **12**, 100550.

Brown, Kenneth, Houck, Daniel, Maniaci, David C & Westergaard, Carsten 2021 Rapidly recovering wind turbine wakes with dynamic pitch and rotor speed control. In *AIAA Scitech 2021 Forum*, p. 1182.

Churchfield, Matthew J & Sirnivas, Senu 2018 On the effects of wind turbine wake skew caused by wind veer. In *2018 wind energy symposium*, p. 0755.

Dairay, Thibault, Lamballais, Eric, Laizet, Sylvain & Vassilicos, John Christos 2017 Numerical dissipation vs. subgrid-scale modelling for large eddy simulation. *Journal of Computational Physics* **337**, 252–274.

Deskos, G., Laizet, S. & Palacios, R. 2020 Winc3d: A novel framework for turbulence-resolving simulations of wind farm wake interactions. *Wind Energy* **23** (3), 779–794.

Frederik, J. A., Weber, R., Cacciola, S., Campagnolo, F., Croce, A., Bottasso, C. & van Wingerden, J. W. 2020 Periodic dynamic induction control of wind farms: proving the potential in simulations and wind tunnel experiments. *Wind Energy Science* **5** (1), 245–257.

Hansen, K S, Barthelmie, R J, Jensen, L E & Sommer, A 2012 The impact of turbulence intensity and atmospheric stability on power deficits due to wind turbine wakes at horns rev wind farm. *Wind Energy* **15** (1), 183–196.

Hodgkin, A, Laizet, S & Deskos, G 2022 Numerical investigation of the influence of shear and thermal stratification on the wind turbine tip-vortex stability. *Wind Energy* .

Houck, Daniel R 2022 Review of wake management techniques for wind turbines. *Wind Energy* **25** (2), 195–220.

Krogstad, P. & Eriksen, P. E. 2013 "blind test" calculations of the performance and wake development for a model wind turbine. *Renewable energy* **50**, 325–333.

Laizet, Sylvain & Lamballais, Eric 2009 High-order compact schemes for incompressible flows : A simple and efficient method with quasi-spectral accuracy. *Journal of Computational Physics* **228** (16), 5989–6015.

Laizet, Sylvain & Li, Ning 2011 Incompact3d : A powerful tool to tackle turbulence problems with up to O (10 5) computational cores. *International Journal for Numerical Methods in Fluids* **67**, 1735–1757.

Lignarolo, L. E. M., Ragni, D., Scarano, F., Ferreira, C. S. & Van Bussel, G. J. W. 2015 Tip-vortex instability and turbulent mixing in wind-turbine wakes. *Journal of Fluid Mechanics* **781**, 467–493.

Munters, Wim & Meyers, Johan 2018*a* Dynamic strategies for yaw and induction control of wind farms based on large-eddy simulation and optimization. *Energies* **11** (1), 177.

Munters, Wim & Meyers, Johan 2018*b* Towards practical dynamic induction control of wind farms: analysis of optimally controlled wind-farm boundary layers and sinusoidal induction control of first-row turbines. *Wind Energy Science* **3** (1), 409–425.

Vermeer, LJ, Sørensen, J N & Crespo, A 2003 Wind turbine wake aerodynamics. *Progress in aerospace sciences* **39** (6-7), 467–510.

Widnall, S. E. 1972 The stability of a helical vortex filament. *Journal of Fluid Mechanics* **54** (4), 641–663.